



UNIVERSITY OF LEEDS

This is a repository copy of *A critical role of TRPM2 channel in A β ₄₂-induced microglial activation and generation of tumor necrosis factor- α .*

White Rose Research Online URL for this paper:
<http://eprints.whiterose.ac.uk/123673/>

Version: Accepted Version

Article:

Mortadza, SAS, Sim, JA, Neubrand, VE et al. (1 more author) (2018) A critical role of TRPM2 channel in A β ₄₂-induced microglial activation and generation of tumor necrosis factor- α . *Glia*, 66 (3). pp. 562-575. ISSN 0894-1491

<https://doi.org/10.1002/glia.23265>

© 2017 Wiley Periodicals, Inc. This is the peer reviewed version of the following article: Alawieyah Syed Mortadza S, Sim JA, Neubrand VE, Jiang L-H. A critical role of TRPM2 channel in A β ₄₂-induced microglial activation and generation of tumor necrosis factor- α . *Glia*. 2018;66:562–575. <https://doi.org/10.1002/glia.23265> , which has been published in final form at <https://doi.org/10.1002/glia.23265>. This article may be used for non-commercial purposes in accordance with Wiley Terms and Conditions for Self-Archiving. Uploaded in accordance with the publisher's self-archiving policy.

Reuse

Items deposited in White Rose Research Online are protected by copyright, with all rights reserved unless indicated otherwise. They may be downloaded and/or printed for private study, or other acts as permitted by national copyright laws. The publisher or other rights holders may allow further reproduction and re-use of the full text version. This is indicated by the licence information on the White Rose Research Online record for the item.

Takedown

If you consider content in White Rose Research Online to be in breach of UK law, please notify us by emailing eprints@whiterose.ac.uk including the URL of the record and the reason for the withdrawal request.



eprints@whiterose.ac.uk
<https://eprints.whiterose.ac.uk/>

A critical role of TRPM2 channel in A β ₄₂-induced microglial activation and generation of tumour necrosis factor- α

Running title: TRPM2 in microglial generation of TNF- α

Sharifah Alawieyah Syed Mortadza^{1,2}, Joan A Sim³, Veronika E Neubrand⁴ and Lin-Hua Jiang^{1,5*}

¹School of Biomedical Sciences, Faculty of Biological Sciences, University of Leeds, UK;

²Faculty of Medicine and Health Science, University Putra Malaysia, Malaysia; ³School of

Medicine, University of Manchester, UK; ⁴Institute of Parasitology and Biomedicine López-

Neyra, Department of Cell Biology and Immunology, IPBLN-CSIC, Avda Conocimiento, PT

Ciencias de La Salud, Granada, Spain; ⁵Sino-UK Joint Laboratory of Brain Function and

Injury of Henan Province and Department of Physiology and Neurobiology, Xinxiang

Medical University, China

*Correspondence: Dr Lin-Hua Jiang (l.h.jiang@leeds.ac.uk), School of Biomedical Sciences,

Faculty of Biological Sciences, University of Leeds, Woodhouse Lane, Leeds LS2 9JT, UK

Author contributions

LHJ conceived the research. LHJ and SSM designed the experiments. SSM performed the experiments. SSM and LHJ analysed the data. JAS and VEN contribute technical assistance and intellectual input into data analysis. LHJ and SSM wrote the manuscript.

Acknowledgements

The work was supported in part by Natural Science Foundation of China (31471118), Alzheimer's Research Trust (ART/PPG2009A/2) and Henan Provincial Department of Education (16IRTSTHN020) to L-HJ. SSM is a recipient of Malaysian Governmental PhD Scholarship. The sponsors played no role in the design and execution of the study.

Conflict of Interest Statement

The authors declare no conflict of interest.

Word Count

Abstract (232); Introduction (705); Materials and Methods (1081); Results (1836); Discussion (862); Figure legends (2254); References (1626); Figures (11); total word count (8918).

Main Points:

- TRPM2 channel is critical for A β ₄₂-induced microglial activation and generation of TNF- α .
- PKC/NOX-mediated ROS generation and activation of the PYK2/MEK/ERK signaling pathway mediate A β ₄₂-induced TRPM2 channel activation.

Abstract

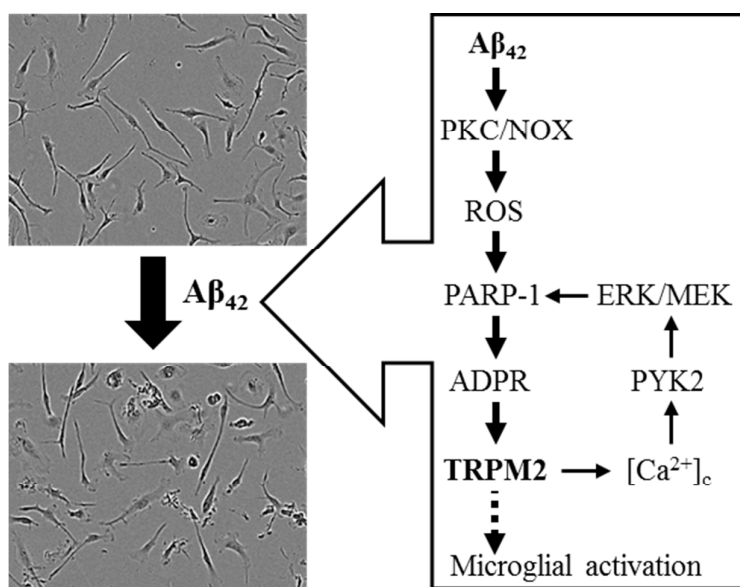
Amyloid β (A β)-induced neuroinflammation plays an important part in Alzheimer's disease (AD). Emerging evidence supports a role for the TRPM2 channel in A β -induced neuroinflammation, but how A β induces TRPM2 channel activation and this relates to neuroinflammation remained poorly understood. We investigated the mechanisms by which A β ₄₂ activates the TRPM2 channel in microglial cells and the relationships to microglial

activation and generation of TNF- α , a key cytokine implicated in AD. Exposure to 10-300 nM A β ₄₂ induced concentration-dependent microglial activation and generation of TNF- α that were ablated by genetically deleting (TRPM2-KO) or pharmacologically inhibiting the TRPM2 channel, revealing a critical role of this channel in A β ₄₂-induced microglial activation and generation of TNF- α . Mechanistically, A β ₄₂ activated the TRPM2 channel via stimulating generation of ROS and activation of PARP-1. A β ₄₂-induced generation of ROS and activation of PARP-1 and TRPM2 channel were suppressed by inhibiting PKC and NADPH oxidases (NOX). A β ₄₂-induced activation of PARP-1 and TRPM2 channel was also reduced by inhibiting PYK2 and MEK/ERK. A β ₄₂-induced activation of PARP-1 was attenuated by TRPM2-KO and moreover, the remaining PARP-1 activity was eliminated by inhibiting PKC and NOX, but not PYK2 and MEK/ERK. Collectively, our results suggest that PKC/NOX-mediated generation of ROS and subsequent activation of PARP-1 play a role in A β ₄₂-induced TRPM2 channel activation and TRPM2-dependent activation of the PYK2/MEK/ERK signalling pathway acts as a positive feedback to further facilitate activation of PARP-1 and TRPM2 channel. These findings provide novel insights into the mechanisms underlying A β -induced AD-related neuroinflammation.

Keywords

A β ₄₂; microglial activation; TNF- α ; TRPM2 channel; ROS; PARP-1

Table of Contents Image



1 INTRODUCTION

Microglial cells, the resident immune cells in the central nervous system (CNS), have an important role in the physiology and diseases of the CNS (Colonna & Butovsky, 2017; Perry & Holmes, 2014; Salter & Beggs, 2014; Tay, Savage, Hui, Bisht, & Tremblay, 2017; Wolf, Boddeke, & Kettenmann, 2017). Under healthy conditions or in the resting state, microglial cells assume a characteristic ramified morphology and perpetually sentinel the surroundings with their fine cell processes. In response to injury or infection, they are transformed to the activated state with an amoeboid morphology and initiate immune response via receptors recognizing danger/pathogen-associated molecular patterns (DAMP/PAMP) molecules to restore normal tissue homeostasis. However, chronic or dysregulated microglial activation and excessive generation of proinflammatory mediators, such as tumour necrosis factor- α (TNF- α) and reactive oxygen species (ROS), can cause neuroinflammation (Colonna & Butovsky, 2017; Regen, Hellmann-Regen, Costantini, & Reale, 2017; Wolf et al., 2017). Accruing preclinical and clinical evidence supports that an increase in amyloid- β peptides (A β) due to an imbalance between generation and removal is an early and initiating factor in Alzheimer's disease (AD), the most common cause of dementia (Hong et al., 2016; Mucke & Selkoe, 2012; Selkoe & Hardy, 2016). It is widely accepted that A β can induce neuroinflammation that contributes to AD (Colonna & Butovsky, 2017; Heneka et al., 2015; Heppner, Ransohoff, & Becher, 2015; Nayak, Roth, & McGavern, 2014; Perry & Holmes, 2014; Prokop, Miller, & Heppner, 2013; Regen et al., 2017; Wolf et al., 2017).

The transient receptor potential melastatin-related 2 (TRPM2) protein forms a Ca²⁺-permeable cationic channel that is gated by intracellular ADP-ribose (ADPR) and also potentially activated by ROS via ADPR-generating mechanisms (Jiang, Yang, Zou, & Beech,

2010). This channel is widely expressed in immune cells and important in normal immune responses and various diseases related to peripheral inflammation (Knowles, Li, & Perraud, 2013; Syed Mortadza, Wang, Li, & Jiang, 2015). A previous study shows that the TRPM2 channel mediates H₂O₂-induced Ca²⁺ influx in monocyte cells that activates the Ca²⁺-sensitive proline-rich tyrosine kinase PYK2 and downstream extracellular signal-regulated kinase (ERK)-dependent signalling pathways to induce generation of chemokine and ulcerative inflammation (Yamamoto et al., 2008). The TRPM2 channel in macrophage cells plays an important role in auto-inflammatory and metabolic diseases by coupling particular crystal/liposome-induced generation of ROS to activation of the NLRP3 inflammasome and generation of interleukin-1 β (Zhong et al., 2013). Several studies examined the role for the TRPM2 channel in macrophage cells in endotoxin-induced generation of TNF- α but the findings are rather specific to particular context or experimental conditions (Di et al., 2011; Haraguchi et al., 2012; Wehrhahn, Kraft, Harteneck, & Hauschildt, 2010).

The expression of TRPM2 channel in microglial cells is also well-documented (Haraguchi et al., 2012; Jeong, Kim, Lee, Jung, & Oh, 2017; Miyake et al., 2014; Mortadza, Sim, Stacey, & Jiang, 2017). Poly(ADPR) polymerase-1 (PARP-1) has a crucial role in ROS-induced generation of ADPR and TRPM2 channel activation (Jiang et al., 2010). There is evidence that activation of PARP-1 is critical in A β -induced microglial activation (Kauppinen et al., 2011). Consistently with these findings, a recent study shows that genetic knockout of the TRPM2 expression strongly suppressed microglial activation in the APP/PS1 AD mice (Ostapchenko et al., 2015). However, the mechanisms by which A β peptides, particularly the neurotoxic A β ₄₂, activate the TRPM2 channel and its relationship to neuroinflammation remained poorly defined. TNF- α is a major neurotoxic cytokine generated by microglial cells (Block, Zecca, & Hong, 2007; Doll, Rellick, Barr, Ren, & Simpkins, 2015; Heppner et al.,

2015; Krabbe et al., 2017; Sedger & McDermott, 2014). Furthermore, studies have reported that generation of TNF- α is increased prior to development of the histopathological hallmarks and co-localized with amyloid plaques in the AD mice and patients, and long-term expression of TNF- α leads to neuronal death in the AD mice; these findings strongly support critical involvement of TNF- α in A β -induced neuroinflammation and AD (Liu & Hong, 2003; Montgomery et al., 2011; Montgomery et al., 2013; Wyss-Coray & Rogers, 2012). In the present study, we investigated the role of the TRPM2 channel in A β ₄₂-induced microglial activation and generation of TNF- α in microglial cells and the signalling mechanisms, through which A β ₄₂ induces TRPM2 channel activation. Our findings provide novel insights into the mechanisms underlying A β -induced neuroinflammation.

2 MATERIALS AND METHODS

2.1 Materials

All chemicals or reagents were obtained from Sigma-Aldrich unless specified otherwise. PJ34 was from Santa Cruz, DPQ from Calbiochem, GKT137831 and U0126 from Cayman Chemical, and CTC and PF431396 from Tocris, respectively. A β ₄₂ and A β ₄₂₋₁ were from Eurogentec and ChinaPeptides. Stock solutions were prepared according to the manufactures' recommendations, aliquoted and kept at -20°C.

2.2 Microglial cell preparation

All experimental protocols, including those using mice, were approved by the University of Leeds Ethical Review Committee and carried out in accordance with the University of Leeds guidelines and procedure and conforming to the UK Home Office regulations. The TRPM2 knockout (TRPM2-KO) mice were generated in our previous study (Zou et al., 2013). Microglia cells were isolated from 1-3 day old wild-type (WT) and TRPM2-KO C57BL/6

mice as detailed in our recent study (Mortadza et al., 2017). Cells were seeded in wells of 96-wells plates (Costar) at a density of 1.1×10^5 , 2.75×10^5 and 3.5×10^5 cells/ml for cell death, Ca^{2+} and ROS imaging, and ELISA assays, respectively, and on poly-L-lysine coated coverslips at 5×10^4 cells/ml in wells of 24-well plates (Costar) for immunostaining. Cells were maintained in DMEM supplemented with 10% foetal bovine serum, 10 units/ml penicillin and 100 $\mu\text{g}/\text{ml}$ streptomycin at 37°C in a humidified atmosphere of 5% CO_2 for 48 hr before use.

2.3 Cell morphology characterization

This was performed 24 hr after cells were exposed to $\text{A}\beta$ peptides ($\text{A}\beta_{42}$ or $\text{A}\beta_{42-1}$) at indicated concentrations. Images were captured using an Incucyte imaging system with a 10x object lens or an EVOS Cell Imaging System with a 40x object lens (Thermo Fisher Scientific). The cell morphology was characterized by computer-assisted analysis of form factor and aspect ratio of individual cells as described in previous studies (Soltys, Ziaja, Pawlinski, Setkowicz, & Janeczko, 2001; Zanier, Fumagalli, Perego, Pischiutta, & De Simoni, 2015). The form factor was calculated as reciprocal of circularity using the formula of $4\pi \times \text{area}/\text{perimeter}^2$, with the highest value of 1.0 indicating a perfect circle and with value approaching 0 indicating an elongated shape. The aspect ratio is defined as the length-to-width ratio, with the minimal value of 1.0 indicating a perfect circle. In experiments examining the effects of inhibitors, cells were treated at 37°C with indicated concentrations of inhibitors 30 min prior to and during exposure to $\text{A}\beta_{42}$.

2.4 Immunofluorescent imaging

Cells were fixed with 4% paraformaldehyde dissolved in deionized water for 15 min and permeabilized in phosphate buffer saline (PBS) containing 0.1% Triton X-100. Following

rinsing with PBS containing 0.5% Tween-20, cells were incubated in PBS containing 5% goat serum for 30 min. Cells were incubated with primary mouse anti-TNF- α (Millipore) at a dilution of 1:400 or anti-PAR antibody (Enzo) at 1:500 overnight at room temperature and, after extensive washing in PSBT, incubated with secondary fluorescein isothiocyanate-conjugated anti-mouse IgG antibody (Sigma; 1:1000) for 1 hr at room temperature. After washing with PBS and rinsing in water, coverslips were mounted using mounting reagent containing 4',6-diamidino-2-phenylindole (DAPI) (Life Technologies). Images were captured using an EVOS Cell Imaging System.

2.5 Enzyme-linked immunosorbent (ELISA) assay of TNF- α release

Cells in 96-well plates were incubated within 50 μ l fresh culture media containing A β ₄₂ at indicated concentrations for 72 hr and the culture media were collected. The TNF- α concentrations in culture media was determined by TNF- α ELISA kits according to the manufacturer's instructions (Peprotech). In experiments studying the effects of inhibitors, cells were treated with the inhibitor at indicated concentrations at 37°C 30 min before and during exposure to A β ₄₂.

2.6 Necrotic cell death assay

This was performed using propidium iodide (PI) staining. Cells in 96-wells plates were treated with A β ₄₂ at indicated concentrations for 72 hr, and were co-stained by PI and Hoechst 33342 (Cell Signaling Technology) with a final concentration of 2 μ g/ml and 5 μ g/ml, respectively. Images were captured using an EVOS Cell Imaging System and analyzed using ImageJ. Cell death was determined by PI-stained cells as percentage of Hoechst-stained cells in three randomly chosen areas in each image.

2.7 Single cell Ca²⁺ imaging

Cells in 96-well plates were treated with A β peptides (A β ₄₂ or A β ₄₂₋₁) at indicated concentrations for 8 hr. Cells were loaded with 5 μ g/ml Fluo4/AM (Life Technologies) at room temperature in standard bath solution (SBS in mM: 134 NaCl, 5 KCl, 0.6 MgCl₂, 1.5 CaCl₂, 8 glucose and 10 HEPES, pH 7.4) as described in our recent study (Mortadza et al., 2017). At the end of Fluo4/AM loading, cells were counterstained by 5 μ g/ml Hoechst. Images were captured using an EVOS Cell Imaging System. Ca²⁺ free-SBS was used in some experiments. In experiments examining the effects of inhibitors, cells were treated at 37°C with the inhibitors at indicated concentrations, 30 min prior to and duration exposure to A β ₄₂.

2.8 Measurement of ROS generation

Cellular ROS generation was assayed using 2',7'-dichlorodihydrofluorescein diacetate (DCFH-DA) as recently described (Mortadza et al., 2017) or Cell-ROX Deep Red (Invitrogen). Briefly, cells plated in 96-well plates were treated with A β ₄₂ at indicated concentrations for 8 hr. Cells were washed with SBS before loaded with 20 μ M DCFH-DA or 5 μ M Cell-ROX Deep Red in SBS at 37°C for 30 min. At the end of staining, cells were counterstained with Hoechst at a final concentration of 5 μ g/ml for 30 min. Images were captured using an EVOS Cell Imaging System. In experiments studying the effects of inhibitors, cells were treated with inhibitors at 37°C 30 min prior to and during exposure to A β ₄₂.

2.9 Data acquisition, presentation and statistical analysis

All the experiments were performed using three to four independent cell preparations, in triplicates (three wells of cells) for each condition each time. For single cell imaging, images of five areas in each well were captured by the EVOS system with fixed exposure time (500

ms) and light intensity (70% illumination), except the experiments shown in figure 10 examining TRPM2-KO cells, where images were captured using 80% illumination, and 75-100 cells were examined in each well. The fluorescence intensity in each cell was quantified using ImageJ and subtracted with the background fluorescence intensity in the same image. The data, where appropriately, are presented as mean \pm standard error of mean (SEM) of the mean values from each independent experiment for each condition. Statistical analysis was performed using Student's t-test for comparison between two groups and one-way ANOVA followed by post hoc Tukey's test for comparison among multiple groups, with $p < 0.05$ being significant.

3 RESULTS

3.1 A β_{42} -induced microglial activation and generation of TNF- α are TRPM2-dependent

A majority of microglial cells in culture displayed a ramified rod-like morphology and a small number of cells a more ramified morphology with more extensive cell processes (Figure 1a), similar to what was previously reported (Lai, Dibal, Armitage, Winship, & Todd, 2013). Exposure to an increasing concentration of A β_{42} (10-300 nM) induced more microglial cells to adopt a morphology typically bearing a single large lamellipodia together with larger amoeboid forms, or larger somata and shorter and coarser processes (Figure 1a). To quantitatively evaluate such A β_{42} -induced effects, we performed computer-assisted analysis of form factor and aspect ratio (as described in Materials and Methods), two geometric parameters commonly used to characterize cell morphology (Soltys et al., 2001; Zanier et al., 2015). Both parameters exhibited widespread distribution (Figure 1b), indicating heterogeneity in cell morphology. Nonetheless, it is evident that the mean value of aspect

ratio was progressively reduced, whereas the mean value of form factor increased, with the $A\beta_{42}$ concentration increasing (Figure 1c). In contrast with the noticeable change in cell morphology induced by 300 nM $A\beta_{42}$, exposure to 300 nM $A\beta_{42-1}$, a peptide with reversal amino acid sequence used as a negative control, resulted in no effect on cell morphology (Figure 1d and supplementary Figure 1). As introduced above, TNF- α represents the major proinflammatory cytokine generated by microglial cells and $A\beta$ -induced generation of TNF- α plays an important role in AD-related neuroinflammation. We therefore performed immunofluorescent imaging to examine TNF- α expression in individual microglial cells 48 hr, and ELISA assay to determine TNF- α release into the culture medium 72 hr, after exposure to $A\beta_{42}$. Exposure to 10-300 nM $A\beta_{42}$ induced a concentration-dependent increase in both TNF- α expression (Figure 1e-f) and TNF- α release by WT microglial cells (Figure 1g). Taken together, these results provide clear evidence to demonstrate that $A\beta_{42}$ at pathologically relevant concentrations induces microglial activation and generation of TNF- α .

Previous studies provide evidence to support that activation of PARP-1 is critical for $A\beta$ -induced or traumatic brain injury-induced microglial activation (Kauppinen et al., 2011; Stoica et al., 2014) and also for ROS-induced TRPM2 channel activation (Jiang et al., 2010). Furthermore, a recent study shows that TRPM2-KO prevented $A\beta$ -induced microglial activation in the APP/PS1 AD mice (Ostapchenko et al., 2015). It is somewhat anticipated but yet there was no evidence to show that the TRPM2 channel plays a role in $A\beta_{42}$ -induced microglial activation. We therefore examined the effects of TRPM2-KO and pharmacological inhibition of the TRPM2 channel on $A\beta_{42}$ -induced microglial activation. There was no difference in microglial cells isolated from WT and TRPM2-KO mice as reported in our previous study (Ye et al., 2014), displaying very similar ramified rod-like morphology (Figure 2a-c). In stark contrast with the remarkable change in the morphology of WT

microglial cells, exposure to A β ₄₂ up to 300 nM induced no significant change in the morphology of TRPM2-KO microglial cells (Figure 2a-c). A β ₄₂-induced change in the morphology of WT microglial cells was prevented with treatment, prior to and during exposure to A β ₄₂, with 100 μ M 2-APB, a TRPM2 channel inhibitor or 1 μ M PJ34, a PARP inhibitor (Jiang et al., 2010). These results from genetic and pharmacological interventions provide consistent evidence to show a critical role for the TRPM2 channel in determining A β ₄₂-induced microglial activation.

We were prompted to investigate whether the TRPM2 channel was also required for A β ₄₂-induced generation of TNF- α . As described above, exposure to 30-300 nM A β ₄₂ induced a strong and concentration-dependent increase in the TNF- α expression in WT microglial cells, but the same treatment induced no detectable increase in the TNF- α expression in TRPM2-KO microglial cells (Figure 3a-b). Consistently, there was no A β ₄₂-induced TNF- α release from TRPM2-KO microglial cells (Figure 3c). A β ₄₂-induced TNF- α release from WT microglial cells was strongly suppressed by treatment with 2-APB, PJ34 or DPQ, another PARP inhibitor (Figure 3d). It has been recently shown that ROS-induced activation of the TRPM2 channel can cause microglial cell death via necrosis (Mortadza et al., 2017). However, PI staining showed that exposure to A β ₄₂ up to 300 nM for 72 hr, the longest treatment used for TNF- α release, induced no significant necrotic cell death (supplementary Figure 2), largely ruling out the possibility that A β ₄₂-induced TNF- α release results from loss of membrane integrity accompanied with necrotic cell death. These results provide compelling evidence to indicate a critical role for the TRPM2 channel in A β ₄₂-induced generation of TNF- α as well as microglial activation.

3.2 A β ₄₂ activates the TRPM2 channel via promoting generation of ROS and activation of PARP-1

To seek mechanistic insights into the TRPM2 channel in A β ₄₂-induced microglial activation and generation of TNF- α , we were interested in the mechanisms by which A β ₄₂ activates the TRPM2 channel. As shown in previous studies (Jeong et al., 2017; Kraft et al., 2004; Miyake et al., 2014; Mortadza et al., 2017), TRPM2 channel activation in microglial cells mediates extracellular Ca²⁺ influx leading to an increase in the [Ca²⁺]_c. We therefore using single cell Ca²⁺ imaging using Fluo4, a fluorescent Ca²⁺ indicator, the method used in our recent study examining Zn²⁺-induced TRPM2 channel activation in microglial cells (Mortadza et al., 2017), to determine whether A β ₄₂ can induce TRPM2 channel activation by monitoring A β ₄₂-induced Ca²⁺ responses. In extracellular Ca²⁺-containing solution, exposure to 10-300 nM A β ₄₂ for 8 hr led to a concentration-dependent increase in the [Ca²⁺]_c (Figure 4a and supplementary Figure 3a), whereas exposure to 300 nM A β ₄₂₋₁ for 8 hr elicited no Ca²⁺ response (supplementary Figure 3b-c). A β ₄₂-induced increase in the [Ca²⁺]_c was not observed in extracellular Ca²⁺-free solution (Figure 4b-c). Furthermore, 30-100 nM A β ₄₂ failed to induce any significant increase in the [Ca²⁺]_c in TRPM2-KO microglial cells (Figure 4d-e). A β ₄₂-induced increase in the [Ca²⁺]_c in WT microglial cells were also abolished by treatment with PJ34 or 2-APB (Figure 4f-g). Taken together, these results consistently support that A β ₄₂ induces TRPM2 channel activation in microglial cells.

We hypothesized that A β ₄₂ induces TRPM2 channel activation via promoting generation of ROS and activation of PARP-1, resulting in generation of ADPR, the TRPM2 channel activator. To testify this hypothesis, we firstly performed single cell imaging using DCF, a fluorescent indicator of cellular ROS. Exposure to 10-300 nM A β ₄₂ for 8 hr led to a salient

and concentration-dependent increase in DCF fluorescence intensity, indicating A β_{42} -induced generation of ROS (Figure 5a-b). Similar results were also obtained using Cell-ROX Deep Red, another fluorescent indicator of cellular ROS (Figure 5c and supplementary Figure 4). Our previous study suggests involvement of the TRPM2 channel in ischemia/reperfusion-induced generation of ROS (Ye et al., 2014). Here, we examined the role of TRPM2 channel in A β_{42} -induced generation of ROS in microglial cells. A β_{42} -induced generation of ROS was significantly reduced but not completely abolished by TRPM2-KO (supplementary Figure 5). We next examined A β_{42} -induced activation of PARP-1 by immunofluorescent imaging of poly(ADPR) or PAR, the product of PARP-1. Exposure to 100 nM A β_{42} resulted in massive generation of PAR in WT microglial cells, which was predominantly concentrated in the nucleus as illustrated by co-localization with DAPI counterstaining (Figure 5d-e). These observations are highly consistent with engagement of PARP-1, the major PARP isoform in the nucleus (Kauppinen & Swanson, 2007). A β_{42} also induced generation of considerable PAR in TRPM2-KO microglial cells, which was however significantly lower than that in WT microglial cells (Figure 5f-g). As anticipated, generation of PAR in both WT and TRPM2-KO cells was completely prevented by treatment with PJ34, prior to and during exposure to A β_{42} (Figure 5f-g). These results, taken together with the above-described observation that A β_{42} -induced TRPM2-mediated increase in the $[Ca^{2+}]_c$ was abolished by treatment with PJ34 (Figure 4), support that A β_{42} activates the TRPM2 channel via inducing generation of ROS and subsequent activation of PARP-1.

3.3 PKC/NOX-mediated generation of ROS is critical in A β_{42} -induced TRPM2 channel activation, microglial activation and generation of TNF- α

NADPH oxidases (NOX) in microglial cells have a significant role in generation of ROS in AD and other neurodegenerative conditions (Block et al., 2007; Cheret et al., 2008; Harrigan, Abdullaev, Jour'dheuil, & Mongin, 2008). Microglial cells are shown to express NOX1, NOX2 and NOX4 (Cheret et al., 2008; Harrigan et al., 2008). In addition, protein kinase C (PKC) and NOX have been reported for ganglioside-induced microglial activation (Min et al., 2004) and microglial cell death after prolonged exposure to Zn^{2+} (Mortadza et al., 2017). We were interested in, and used the same treatments described in our recent study to examine whether PKC and NOX were importantly involved in $A\beta_{42}$ -induced generation of ROS that leads to activation of PARP-1 and TRPM2 channel. Treatment, prior to and duration exposure to $A\beta_{42}$, with 3 μ M CTC, a PKC inhibitor, or 3 μ M DPI, a generic NOX inhibitor, 3 μ M GKT, a NOX1/4 inhibitor or 30 μ M Phox, a NOX2 inhibitor, strongly inhibited $A\beta_{42}$ -induced generation of ROS (Figure 6a and d), activation of PARP-1 (Figure 6b and e) and TRPM2-mediated increase in the $[Ca^{2+}]_c$ (Figure 6c and f). Such treatments also blocked $A\beta_{42}$ -induced microglial activation (Figure 7a-d). Furthermore, treatment with 1-3 μ M CTC, DPI or GKT and 30 μ M Phox strongly suppressed $A\beta_{42}$ -induced generation of TNF- α (Figure 7e). These results thus strongly indicate a critical role for PKC/NOX in $A\beta_{42}$ -induced generation of ROS and activation of PARP-1 and TRPM2 channel, providing further evidence to support the role of TRPM2 channel in $A\beta_{42}$ -induced microglial activation and generation of TNF- α .

3.4 The PYK2/MEK/ERK signalling pathway acts a positive feedback in $A\beta_{42}$ -induced activation of PARP-1 and TRPM2 channel, microglial activation and generation of TNF- α

TRPM2-mediated Ca^{2+} influx was previously showed to activate the PYK2/MEK/ERK pathway in ROS-induced generation of chemokine by monocyte cells (Yamamoto et al.,

2008). We moved to examine whether such a signalling pathway participated in A β_{42} -induced microglial activation and generation of TNF- α . Treatment with 1 μ M PF, a PYK2 inhibitor, or 3 μ M U0126, a MEK/ERK inhibitor, largely prevented A β_{42} -induced microglial activation (Figure 8a-b). In addition, treatment with 0.1-1 μ M PF or 1-3 μ M U0126 strongly inhibited A β_{42} -induced generation of TNF- α (Figure 8c). These results provide clear evidence to suggest that the PYK2/MEK/ERK signalling pathway is important in A β_{42} -induced microglial activation and generation of TNF- α .

It is known that activation of ERK can stimulate the PARP-1 activity (Domercq et al., 2013; Kauppinen et al., 2006). Treatment with 1 μ M PF or 3 μ M U0126 strongly inhibited A β_{42} -induced activation of PARP-1 (Figure 9a-b) and TRPM2-mediated increase in the $[Ca^{2+}]_c$ (Figure 9c-d), supporting a role for the PYK2/MEK/ERK signalling pathway in A β_{42} -induced activation of PARP-1 and TRPM2 channel. We have recently reported that activation of this signalling pathway serves as a positive feedback mechanism to facilitate activation of PARP-1 and TRPM2 channel in microglial cell death induced by prolonged exposure to Zn²⁺ (Mortadza et al., 2017). A β_{42} -induced activation of PARP-1 in TRPM2-KO microglial cells was blunted by inhibiting PKC with CTC or NOX with DPI, GKT or Phox (Figure 10a-d), but unaffected by blocking PYK2 or MEK/ERK with PF and U0126, respectively (Figure 10e-f). These results are consistent with the notion that the PYK2/MEK/ERK signalling pathway as a mechanism downstream of the TRPM2 channel further enhances activation of PARP-1 and TRPM2 channel (Figure 11).

4 DISCUSSION

Our study provides evidence to demonstrate a critical role for the TRPM2 channel in A β_{42} -induced microglial activation and generation of TNF- α . We show that PKC/NOX-mediated

generation of ROS and activation of PARP-1 are required for A β ₄₂-induced TRPM2 channel activation and, furthermore, the PYK2/MEK/ERK signalling pathway as a positive feedback mechanism downstream of TRPM2 channel activation facilitates further activation of PARP-1 and TRPM2 channel (Figure 11). These molecular and signalling mechanisms are also important in A β ₄₂-induced microglial activation and generation of TNF- α . Our findings thus provide novel insights into the mechanisms underlying A β -induced neuroinflammation.

It has been well recognized that A β causes neuroinflammation via inducing microglial activation and generation of excessive proinflammatory cytokines, thereby contributing to AD (Heneka et al., 2015; Heppner et al., 2015). Here we confirmed that A β ₄₂ at pathologically relevant concentrations induced microglial activation (Figure 1a-d). In addition, A β ₄₂-induced microglial activation (Figure 2d-e) and generation of nuclear PAR (Figure 5e-f) were strongly inhibited by PJ34, consistent with the reported role of PARP-1 in A β -induced microglial activation (Kauppinen et al., 2011). In this study, we further showed that A β ₄₂-induced microglial activation was prevented by TRPM2-KO (Figure 2a-c) or inhibition of the TRPM2 channel (Figure 2d-e). These observations, together with a recent finding that TRPM2-KO suppressed microglial activation in the APP/PS1 AD mice (Ostapchenko et al., 2015), strongly support a critical role for the TRPM2 channel in A β ₄₂-induced microglial activation.

A β -induced microglial activation via activating the TRPM2 channel has been implicated in AD (Ostapchenko et al., 2015), but evidence supporting the role for the TRPM2 channel in A β -induced neuroinflammation is still lacking. As introduced above, it has been well-documented that TNF- α is potent in inducing neurotoxicity and that A β -induced generation of TNF- α from microglial cells significantly contributes to neuroinflammation in AD (Alam

et al., 2016; Block et al., 2007; Doll et al., 2015; Heppner et al., 2015; Krabbe et al., 2017; Liu & Hong, 2003; Montgomery et al., 2011; Montgomery et al., 2013; Wyss-Coray & Rogers, 2012). The present study showed that A β ₄₂ induced generation of TNF- α by microglial cells (Figure 1e-g). Importantly, we showed that such generation was strongly suppressed by TRPM2-KO (Figure 3a-c) and inhibiting the TRPM2 channel with 2-APB, or inhibiting PARP-1 with PJ34 and DPQ (Figure 3d), thus providing compelling evidence for the first time to demonstrate a critical role of the TRPM2 channel in A β ₄₂-induced generation of TNF- α . Considering the well-known neurotoxicity of TNF- α , our finding suggests, although further investigations are required to substantiate, a significant role of A β ₄₂-induced TRPM2-dependent generation of TNF- α in AD pathogenesis.

In the present study, we showed that A β ₄₂ induced TRPM2 channel activation (Figure 4). We further demonstrated that activation of PKC and NOX, including NOX1/4 and NOX2, and NOX-mediated generation of ROS are important in A β ₄₂-induced TRPM2 channel activation (Figure 6) as well as microglial activation and generation of TNF- α (Figure 7). Activation of these molecular mechanisms has been recently shown to be vital in TRPM2 channel activation induced by prolonged exposure to Zn²⁺ (Mortadza et al., 2017). Two recent studies have reported that LPS/IFN γ and LPC can induce TRPM2 channel activation but the activation mechanisms remain to be established (Jeong et al., 2017; Miyake et al., 2014). Regardless, the previous and present studies provide increasing evidence to support a widespread role for the TRPM2 channel in coupling diverse DAMP/PAMP molecules to an increase in the [Ca²⁺]_c in microglial cells. A previous study shows that TRPM2-mediated Ca²⁺ influx in monocyte cells activates the PYK2/MEK/ERK signalling pathway in ROS-induced generation of chemokine (Yamamoto et al., 2008). Our recent study suggests such a signalling pathway acts as a positive feedback mechanism downstream of the TRPM2

channel to further enhance activation of PARP-1 and TRPM2 channel in microglial cells in response to prolonged exposure to Zn^{2+} (Mortadza et al., 2017). In the present study, we showed that the PYK2/MEK/ERK signalling pathway is also critical in $A\beta_{42}$ -induced microglial activation and generation of $TNF-\alpha$ (Figure 8) as well as TRPM2 channel activation in microglial cells (Figure 9). TRPM2-KO significantly attenuated but did not completely prevent $A\beta_{42}$ -induced generation of ROS (supplementary figure 5), as previously reported in ischemia/reperfusion-induced generation of ROS in hippocampal neurons (Ye et al., 2014). Further investigations are required to understand the underlying mechanisms. Similarly, $A\beta_{42}$ -induced activation of PARP-1 depends on the TRPM2 channel because TRPM2-KO also significantly reduced $A\beta_{42}$ -induced activation of PARP-1 (Figure 5f-g). The remaining $A\beta_{42}$ -induced PARP-1 activity in TRPM2-KO microglial cells was totally abolished by inhibiting PKC/NOX (Figure 10a-d) but not PYK2/MEK/ERK (Figure 10e-f). These differentiating results support the notion that $A\beta_{42}$ -induced PKC/NOX-mediated generation of ROS and activation of PARP-1 plays a significant role in initiating TRPM2 channel activation and subsequently the PYK2/MEK/ERK signalling pathway is fed back to activation of PARP-1 to further enhance TRPM2 channel activation (Figure 11).

In conclusion, we show a critical role for the TRPM2 channel in $A\beta_{42}$ -induced microglial activation and generation of $TNF-\alpha$. We further reveal that PKC/NOX-mediated generation of ROS and activation of PARP-1 are required for $A\beta_{42}$ -induced TRPM2 channel activation and the PYK2/MEK/ERK signalling pathway as a positive feedback mechanism further stimulates activation of PARP-1 and TRPM2 channel. These novel findings provide mechanistic insights into $A\beta$ -induced neuroinflammation in AD pathogenesis.

References

Alam, Q., Alam, M. Z., Mushtaq, G., Damanhour, G. A., Rasool, M., Kamal, M. A., & Haque, A. (2016). Inflammatory Process in Alzheimer's and Parkinson's Diseases: Central Role of Cytokines. *Current Pharmaceutical Design*, *22*, 541-548.

Block, M. L., Zecca, L., & Hong, J. S. (2007). Microglia-mediated neurotoxicity: uncovering the molecular mechanisms. *Nature Review Neuroscience*, *8*, 57-69. doi: 10.1038/nrn2038

Cheret, C., Gervais, A., Lelli, A., Colin, C., Amar, L., Ravassard, P., . . . Mallat, M. (2008). Neurotoxic activation of microglia is promoted by a nox1-dependent NADPH oxidase. *Journal of Neuroscience*, *28*, 12039-12051. doi: 10.1523/JNEUROSCI.3568-08.2008

Colonna, M., & Butovsky, O. (2017). Microglia function in the central nervous system during health and neurodegeneration. *Annual Review of Immunology*, *35*, 441-468. doi: 10.1146/annurev-immunol-051116-052358

Di, A., Gao, X. P., Qian, F., Kawamura, T., Han, J., Hecquet, C., . . . Malik, A. B. (2011). The redox-sensitive cation channel TRPM2 modulates phagocyte ROS production and inflammation. *Nature Immunology*, *13*, 29-34. doi: 10.1038/ni.2171

Doll, D. N., Rellick, S. L., Barr, T. L., Ren, X., & Simpkins, J. W. (2015). Rapid mitochondrial dysfunction mediates TNF-alpha-induced neurotoxicity. *Journal of Neurochemistry*, *132*, 443-451. doi: 10.1111/jnc.13008

Domercq, M., Mato, S., Soria, F. N., Sanchez-gomez, M. V., Alberdi, E., & Matute, C. (2013). Zn²⁺-induced ERK activation mediates PARP-1-dependent ischemic-reoxygenation damage to oligodendrocytes. *Glia*, *61*, 383-393. doi: 10.1002/glia.22441

Haraguchi, K., Kawamoto, A., Isami, K., Maeda, S., Kusano, A., Asakura, K., . . . Kaneko, S. (2012). TRPM2 contributes to inflammatory and neuropathic pain through the aggravation of pronociceptive inflammatory responses in mice. *Journal of Neuroscience*, *32*, 3931-3941. doi: 10.1523/JNEUROSCI.4703-11.2012

- Harrigan, T. J., Abdullaev, I. F., Jourd'heuil, D., & Mongin, A. A. (2008). Activation of microglia with zymosan promotes excitatory amino acid release via volume-regulated anion channels: the role of NADPH oxidases. *Journal of Neurochemistry*, *106*, 2449-2462. doi: 10.1111/j.1471-4159.2008.05553.x
- Heneka, M. T., Carson, M. J., El Khoury, J., Landreth, G. E., Brosseron, F., Feinstein, D. L., . . . Kummer, M. P. (2015). Neuroinflammation in Alzheimer's disease. *Lancet Neurology*, *14*, 388-405. doi: 10.1016/S1474-4422(15)70016-5
- Heppner, F. L., Ransohoff, R. M., & Becher, B. (2015). Immune attack: the role of inflammation in Alzheimer disease. *Nature Review Neuroscience*, *16*, 358-372. doi: 10.1038/nrn3880
- Hong, S., Beja-Glasser, V. F., Nfonoyim, B. M., Frouin, A., Li, S., Ramakrishnan, S., . . . Stevens, B. (2016). Complement and microglia mediate early synapse loss in Alzheimer mouse models. *Science*, *352*, 712-716. doi: 10.1126/science.aad8373
- Jeong, H., Kim, Y. H., Lee, Y., Jung, S. J., & Oh, S. B. (2017). TRPM2 contributes to LPC-induced intracellular Ca²⁺ influx and microglial activation. *Biochemical and Biophysical Research Communications*, *485*, 301-306. doi: 10.1016/j.bbrc.2017.02.087
- Jiang, L. H., Yang, W., Zou, J., & Beech, D. J. (2010). TRPM2 channel properties, functions and therapeutic potentials. *Experts Opinion on Therapeutic Targets*, *14*, 973-988. doi: 10.1517/14728222.2010.510135
- Kauppinen, T. M., Chan, W. Y., Suh, S. W., Wiggins, A. K., Huang, E. J., & Swanson, R. A. (2006). Direct phosphorylation and regulation of poly(ADP-ribose) polymerase-1 by extracellular signal-regulated kinases 1/2. *Proceedings of the National Academy of Sciences of the United States of America*, *103*, 7136-7141. doi: 10.1073/pnas.0508606103

- Kauppinen, T. M., Suh, S. W., Higashi, Y., Berman, A. E., Escartin, C., Won, S. J., . . . Swanson, R. A. (2011). Poly(ADP-ribose) polymerase-1 modulates microglial responses to amyloid beta. *Journal of Neuroinflammation*, *8*, 152. doi: 10.1186/1742-2094-8-152
- Kauppinen, T. M., & Swanson, R. A. (2007). The role of poly(ADP-ribose) polymerase-1 in CNS disease. *Neuroscience*, *145*, 1267-1272. doi: 10.1016/j.neuroscience.2006.09.034
- Knowles, H., Li, Y., & Perraud, A. L. (2013). The TRPM2 ion channel, an oxidative stress and metabolic sensor regulating innate immunity and inflammation. *Immunological Research*, *55*, 241-248. doi: 10.1007/s12026-012-8373-8
- Krabbe, G., Minami, S. S., Etcheagaray, J. I., Taneja, P., Djukic, B., Davalos, D., . . . Gan, L. (2017). Microglial NFkappaB-TNFalpha hyperactivation induces obsessive-compulsive behavior in mouse models of progranulin-deficient frontotemporal dementia. *Proceedings of the National Academy of Sciences of the United States of America*, *114*, 5029-5034. doi: 10.1073/pnas.1700477114
- Kraft, R., Grimm, C., Grosse, K., Hoffmann, A., Sauerbruch, S., Kettenmann, H., . . . Harteneck, C. (2004). Hydrogen peroxide and ADP-ribose induce TRPM2-mediated calcium influx and cation currents in microglia. *American Journal of Physiology Cell Physiology*, *286*, C129-137. doi: 10.1152/ajpcell.00331.2003
- Lai, A. Y., Dibal, C. D., Armitage, G. A., Winship, I. R., & Todd, K. G. (2013). Distinct activation profiles in microglia of different ages: a systematic study in isolated embryonic to aged microglial cultures. *Neuroscience*, *254*, 185-195. doi: 10.1016/j.neuroscience.2013.09.010
- Liu, B., & Hong, J. S. (2003). Role of microglia in inflammation-mediated neurodegenerative diseases: mechanisms and strategies for therapeutic intervention. *Journal of Pharmacology and Experimental Therapeutics*, *304*, 1-7. doi: 10.1124/jpet.102.035048

Min, K. J., Pyo, H. K., Yang, M. S., Ji, K. A., Jou, I., & Joe, E. H. (2004). Gangliosides activate microglia via protein kinase C and NADPH oxidase. *Glia*, *48*, 197-206. doi: 10.1002/glia.20069

Miyake, T., Shirakawa, H., Kusano, A., Sakimoto, S., Konno, M., Nakagawa, T., . . . Kaneko, S. (2014). TRPM2 contributes to LPS/IFN γ -induced production of nitric oxide via the p38/JNK pathway in microglia. *Biochemical and Biophysical Research Communications*, *444*, 212-217. doi: 10.1016/j.bbrc.2014.01.022

Montgomery, S. L., Mastrangelo, M. A., Habib, D., Narrow, W. C., Knowlden, S. A., Wright, T. W., & Bowers, W. J. (2011). Ablation of TNF-RI/RII expression in Alzheimer's disease mice leads to an unexpected enhancement of pathology: implications for chronic pan-TNF- α suppressive therapeutic strategies in the brain. *American Journal of Pathology*, *179*, 2053-2070. doi: 10.1016/j.ajpath.2011.07.001

Montgomery, S. L., Narrow, W. C., Mastrangelo, M. A., Olschowka, J. A., O'Banion, M. K., & Bowers, W. J. (2013). Chronic neuron- and age-selective down-regulation of TNF receptor expression in triple-transgenic Alzheimer disease mice leads to significant modulation of amyloid- and tau-related pathologies. *American Journal of Pathology*, *182*(6), 2285-2297. doi: 10.1016/j.ajpath.2013.02.030

Mortadza, S. S., Sim, J. A., Stacey, M., & Jiang, L. H. (2017). Signalling mechanisms mediating Zn²⁺-induced TRPM2 channel activation and cell death in microglial cells. *Scientific Reports*, *7*, 45032. doi: 10.1038/srep45032

Mucke, L., & Selkoe, D. J. (2012). Neurotoxicity of amyloid beta-protein: synaptic and network dysfunction. *Cold Spring Harbor Perspectives in Medicine*, *2*, a006338. doi: 10.1101/cshperspect.a006338

- Nayak, D., Roth, T. L., & McGavern, D. B. (2014). Microglia development and function. *Annual Review of Immunology*, *32*, 367-402. doi: 10.1146/annurev-immunol-032713-120240
- Ostapchenko, V. G., Chen, M., Guzman, M. S., Xie, Y. F., Lavine, N., Fan, J., . . . Jackson, M. F. (2015). The transient receptor potential melastatin 2 (TRPM2) channel contributes to beta-amyloid oligomer-related neurotoxicity and memory impairment. *Journal of Neuroscience*, *35*, 15157-15169. doi: 10.1523/JNEUROSCI.4081-14.2015
- Perry, V. H., & Holmes, C. (2014). Microglial priming in neurodegenerative disease. *Nature Review Neurology*, *10*, 217-224. doi: 10.1038/nrneurol.2014.38
- Prokop, S., Miller, K. R., & Heppner, F. L. (2013). Microglia actions in Alzheimer's disease. *Acta Neuropathology*, *126*, 461-477.
- Regen, F., Hellmann-Regen, J., Costantini, E., & Reale, M. (2017). Neuroinflammation and Alzheimer's disease: implications for microglial activation. *Current Alzheimer Research*. doi: 10.2174/1567205014666170203141717
- Salter, M. W., & Beggs, S. (2014). Sublime microglia: expanding roles for the guardians of the CNS. *Cell*, *158*, 15-24. doi: 10.1016/j.cell.2014.06.008
- Sedger, L. M., & McDermott, M. F. (2014). TNF and TNF-receptors: From mediators of cell death and inflammation to therapeutic giants - past, present and future. *Cytokine and Growth Factor Review*, *25*, 453-472. doi: 10.1016/j.cytogfr.2014.07.016
- Selkoe, D. J., & Hardy, J. (2016). The amyloid hypothesis of Alzheimer's disease at 25 years. *EMBO Molecular Medicine*, *8*, 595-608. doi: 10.15252/emmm.201606210
- Soltys, Z., Ziaja, M., Pawlinski, R., Setkowicz, Z., & Janeczko, K. (2001). Morphology of reactive microglia in the injured cerebral cortex. Fractal analysis and complementary quantitative methods. *Journal of Neuroscience Research*, *63*, 90-97. doi: 10.1002/1097-4547(20010101)63:1<90::AID-JNR11>3.0.CO;2-9

- Stoica, B. A., Loane, D. J., Zhao, Z., Kabadi, S. V., Hanscom, M., Byrnes, K. R., & Faden, A. I. (2014). PARP-1 inhibition attenuates neuronal loss, microglia activation and neurological deficits after traumatic brain injury. *Journal of Neurotrauma*, *31*, 758-772. doi: 10.1089/neu.2013.3194
- Syed Mortadza, S. A., Wang, L., Li, D., & Jiang, L. H. (2015). TRPM2 channel-mediated ROS-sensitive Ca²⁺ signaling mechanisms in immune cells. *Frontiers in Immunology*, *6*, 407. doi: 10.3389/fimmu.2015.00407
- Tay, T. L., Savage, J. C., Hui, C. W., Bisht, K., & Tremblay, M. E. (2017). Microglia across the lifespan: from origin to function in brain development, plasticity and cognition. *Journal of Physiology*, *595*, 1929-1945. doi: 10.1113/JP272134
- Wehrhahn, J., Kraft, R., Harteneck, C., & Hauschildt, S. (2010). Transient receptor potential melastatin 2 is required for lipopolysaccharide-induced cytokine production in human monocytes. *Journal of Immunology*, *184*, 2386-2393. doi: 10.4049/jimmunol.0902474
- Wolf, S. A., Boddeke, H. W., & Kettenmann, H. (2017). Microglia in Physiology and Disease. *Annual Review of Physiology*, *79*, 619-643. doi: 10.1146/annurev-physiol-022516-034406
- Wyss-Coray, T., & Rogers, J. (2012). Inflammation in Alzheimer disease—a brief review of the basic science and clinical literature. *Cold Spring Harbor Perspectives in Medicine*, *2*, a006346. doi: 10.1101/cshperspect.a006346
- Yamamoto, S., Shimizu, S., Kiyonaka, S., Takahashi, N., Wajima, T., Hara, Y., . . . Mori, Y. (2008). TRPM2-mediated Ca²⁺-influx induces chemokine production in monocytes that aggravates inflammatory neutrophil infiltration. *Nature Medicine*, *14*, 738-747. doi: 10.1038/nm1758
- Ye, M., Yang, W., Ainscough, J. F., Hu, X. P., Li, X., Sedo, A., . . . Jiang, L. H. (2014). TRPM2 channel deficiency prevents delayed cytosolic Zn²⁺ accumulation and CA1

pyramidal neuronal death after transient global ischemia. *Cell Death and Diseases*, 5, e1541.

doi: 10.1038/cddis.2014.494

Zanier, E. R., Fumagalli, S., Perego, C., Pischiutta, F., & De Simoni, M. G. (2015). Shape descriptors of the "never resting" microglia in three different acute brain injury models in mice. *Intensive Care Medicine Experimental*, 3, 39. doi: 10.1186/s40635-015-0039-0

Zhong, Z., Zhai, Y., Liang, S., Mori, Y., Han, R., Sutterwala, F. S., & Qiao, L. (2013). TRPM2 links oxidative stress to NLRP3 inflammasome activation. *Nature Communication*, 4, 1611. doi: 10.1038/ncomms2608

Zou, J., Ainscough, J. F., Yang, W., Sedo, A., Yu, S. P., Mei, Z. Z., . . . Jiang, L. H. (2013). A differential role of macrophage TRPM2 channels in Ca^{2+} signaling and cell death in early responses to H_2O_2 . *American Journal of Physiology Cell Physiology*, 305, C61-69. doi: 10.1152/ajpcell.00390.2012

Figure Legend

Fig. 1 $\text{A}\beta_{42}$ induces morphological changes and generation of $\text{TNF-}\alpha$ in microglial cells

(a) Representative phase-contrast images showing microglial cell morphology in culture without (CTL) or with exposure to $\text{A}\beta_{42}$ at indicated concentrations for 24 hr, captured using an Incucyte imaging system with a 10x object lens (top) and an EVOS imaging system with a 40x object lens (bottom). (b, c) Scatter plot showing the distribution of form factor and aspect ratio values of individual microglial cells (b), and mean form factor (top) and aspect ratio (bottom) values for microglial cells treated with the conditions shown in (a), from 4 independent cell preparations. (d) Mean form factor (top) and aspect ratio (bottom) values of microglial cells without or with exposure to 300 nM $\text{A}\beta_{42}$ or 300 nM $\text{A}\beta_{42-1}$ for 24 hr, from 3 independent cell preparations. (e) Representative immunofluorescent images showing $\text{TNF-}\alpha$ expression in individual microglial cells without (CTL) and with exposure to $\text{A}\beta_{42}$ at

indicated concentrations for 48 hr. Cells were counterstained with DAPI. (f) Summary of TNF- α expression in microglial cells under the conditions shown in (e), from 3 independent cell preparations. (g) Summary of TNF- α release determined by ELISA from microglial cells after exposed to A β ₄₂ at indicated concentrations for 72 hr from 4 independent cell preparations. Scale bar: 200 μ m (a, top), 50 μ m (a, bottom) and 40 μ m (e). *, p < 0.05; **, p < 0.01; ***, p < 0.005 compared to control.

Fig. 2 TRPM2 is required for A β ₄₂-induced microglial activation

(a) Representative phase-contrast images showing single cell morphology of WT and TRPM2-KO microglial cells without (CTL) or with exposure to A β ₄₂ at indicated concentrations for 24 hr, captured using an EVOS imaging system with a 40x object lens. (b, c) Scatter plot showing the distribution of form factor and aspect ratio values of individual microglial cells (b), and mean form factor (top) and aspect ratio (bottom) values for microglial cells under the conditions indicated in (a), from 4 independent cell preparations. (d, e) Scatter plot showing the distribution of form factor and aspect ratio values of individual WT microglial cells (d), and mean form factor (left) and aspect ratio (right) values for microglial cells without (CTL) or with exposure to 100 nM A β ₄₂ for 24 hr alone or treatment with 1 μ M PJ-34 or 100 μ M 2-APB, 30 min prior to and duration exposure to A β ₄₂ (e), from 4 independent cell preparations. Scale bar: 50 μ m. ***, p < 0.005 compared to control. ###, p < 0.005 compared between WT and TRPM2-KO cells under the same treatment (c), or compared to cells exposed to A β ₄₂ alone (e).

Fig. 3 TRPM2 is important for A β ₄₂-induced generation of TNF- α by microglial cells

(a) Representative immunofluorescent images showing TNF- α expression in individual microglial cells from WT and TRPM2-KO mice without (CTL) or with exposure to A β ₄₂ at

indicated concentrations for 48 hr. Cells were counterstained with DAPI. **(b)** Summary of TNF- α expression in microglial cells under the conditions indicated in (a), from 3 independent cell preparations. **(c)** Summary of TNF- α release determined by ELISA from WT and TRPM2-KO microglial cells without or with exposure to A β ₄₂ at indicated concentrations for 72 hr, from 4 independent cell preparations. **(d)** Summary of TNF- α release from microglial cells after exposure to 100 nM A β ₄₂ for 72 hr alone or treatment with 1 μ M PJ-34 or 100 μ M 2-APB, 30 min prior to and during exposure to A β ₄₂, from 3 independent cell preparations. Scale bar: 40 μ m. *, p < 0.05; ***, p < 0.005 compared to control. #, p < 0.05; ##, p < 0.01; ###, p < 0.005 compared between WT and TRPM2-KO cells under the same treatment (b, c) and cells exposed to A β ₄₂ alone (d).

Fig. 4 A β ₄₂ induces Ca²⁺ influx and cytosolic Ca²⁺ increase through TRPM2 channel activation

(a) Summary of the Fluo4 fluorescence intensity, indicative of the cytosolic Ca²⁺ levels, in WT microglial cells without (CTL) or with exposure to A β ₄₂ at indicated concentrations for 8 hr, from 3 independent cell preparations using 3 wells of cells for each condition in each time. **(b, d, f)** Representative single cell Fluo4 fluorescent images showing the cytosolic Ca²⁺ levels (top row: Fluo4 fluorescence; bottom row: counterstaining with Hoechst) in WT microglial cells without (CTL) or with exposure to 100 nM A β ₄₂ for 8 hr in extracellular Ca²⁺-containing (+Ca²⁺) or Ca²⁺-free (-Ca²⁺) solutions (b), in WT and TRPM2-KO microglial cells without (CTL) or with exposure to A β ₄₂ at indicated concentrations (d), or in WT microglial cells after exposure to 100 nM A β ₄₂ for 8 hr alone or treatment with 1 μ M PJ34 or 100 μ M 2-APB, 30 min prior to and during exposure to A β ₄₂ (f). **(c, e, g)** Summary of the mean cytosolic Ca²⁺ levels in microglial cells under conditions indicated in (b, d, f), from 3 independent cell preparations. Scale bar: 40 μ m. *, p < 0.05; ***, p < 0.005 compared to

control. ##, $p < 0.01$; ###, $p < 0.005$ ###, between cells exposed to $A\beta_{42}$ in the presence and absence of Ca^{2+} in extracellular solutions (c), between WT and TRPM2-KO cells under the same treatment (e), or between cells without or with treatment with PJ34 or 2-APB.

Fig. 5 $A\beta_{42}$ induces generation of cellular ROS and activation of PARP-1 in microglial cells

(a) Representative single cell DCF fluorescence images showing cellular ROS generation (top row: DCF fluorescence; bottom row: counterstaining with Hoechst) in microglial cells without (CTL) or with exposure to $A\beta_{42}$ at indicated concentrations for 8 hr. (b) Summary of $A\beta_{42}$ -induced ROS generation in microglial cells under conditions shown in (a), from 3 independent cell preparations. (c) Summary of $A\beta_{42}$ -induced ROS production using Cell-ROX Deep Red in microglial cells under conditions shown in (a), from 3 independent cell preparations. (d, f) Representative immunofluorescent images showing generation of PAR (top row) and counterstaining with DAPI (bottom row) in individual microglial cells without (CTL) or with exposure to 100 nM $A\beta_{42}$ for 8 hr (d), or after exposure to with 100 nM $A\beta_{42}$ for 8 hr alone or treatment with 1 μ M PJ34 in WT and KO-TRPM2 microglial cells, 30 min prior to and during exposure to $A\beta_{42}$ (f). (e, g) Summary of $A\beta_{42}$ -induced generation of PAR in microglial cells under indicated conditions from 3 independent cell preparations. Scale bar: 40 μ m. *, $p < 0.05$; **, $p < 0.01$; ***, $p < 0.005$ compared to control. ##, $p < 0.01$ compared between WT and TRPM2-KO cells under the same treatment.

Fig. 6 PKC and NOX are involved in $A\beta_{42}$ -induced generation of ROS, activation of PARP-1 and TRPM2 channel activation

(a, d) *Left*, representative single cell DCF fluorescence images showing cellular ROS generation (top row: DCF fluorescence; bottom row: counterstaining with Hoechst) in

microglial cells after exposure for 8 hr to 100 nM A β ₄₂ alone or treatment with 3 μ M chelerythrine chloride (CTC) (a), 3 μ M diphenyleneiodonium (DPI), 3 μ M GKT137831 (GKT) or 30 μ M Phox-I2 (Phox) (d). *Right*, summary of A β ₄₂-induced ROS generation in microglial cells under indicated conditions, from 3 independent cell preparations. **(b, e)** *Left*, representative immunofluorescent images showing PAR generation (top row) and counterstaining with DAPI (bottom row) in individual microglial cells after exposure for 8 hr to 100 nM A β ₄₂ alone or treatment with CTC (b), DPI, GKT or Phox (e). *Right*, Summary of A β ₄₂-induced PAR generation in microglial cells under indicated conditions from 3 independent cell preparations. **(c, f)** *Left*, representative single cell Fluo4 fluorescence images showing the cytosolic Ca²⁺ levels in microglial cells treated with indicated conditions (top row: Fluo4 fluorescence; bottom row: counterstaining with Hoechst). *Right*, summary of A β ₄₂-induced Ca²⁺ responses in microglial cells under indicated conditions, from 3 independent cell preparations. Cells were treated with inhibitors, 30 min prior to and during exposure to A β ₄₂. Scale bar: 40 μ m. *******, p < 0.005 compared to control. **###**, p < 0.005 compared to cells exposed to A β ₄₂ alone.

Fig. 7 Activation of PKC and NOX is vital in A β ₄₂-induced microglial activation and generation of TNF- α

(a, c) Scatter plot showing the distribution of form factor and aspect ratio values of individual microglial cells after exposure for 24 hr to 100 nM A β ₄₂ alone or treatment with 3 μ M CTC (a), 3 μ M DPI, 3 μ M GKT or 30 μ M Phox (c), 30 min prior to and during exposure to A β ₄₂. **(b, d)** Summary of the mean form factor (top) and aspect ratio (bottom) values for microglial cells under indicated conditions from 3 independent cell preparations. **(e)** Summary of TNF- α release determined by ELISA from microglial cells without (CTL) or with exposure to 100

nM A β_{42} alone or treatment with inhibitors at indicated concentrations from 3 independent cell preparations. Cells were treated with inhibitors, 30 min prior to and during exposure to A β_{42} . ***, $p < 0.005$ compared to control. ##, $p < 0.01$; ###, $p < 0.005$ compared to cells exposed to A β_{42} alone.

Fig. 8 The PYK2/MEK/ERK signalling pathway is critically involved in A β_{42} -induced microglial cell activation and generation of TNF- α

(a, b) Scatter plot showing the distribution of form factor and aspect ratio values of individual microglial cells (a), or mean form factor (left) and aspect ratio (right) values for microglial cells (b) without (CTL) or with exposure for 24 hr to 100 nM A β_{42} alone or treatment with 1 μ M PF 431396 (PF) or 3 μ M U0126, 30 min prior to and during exposure to A β_{42} , from 3 independent cell preparations. (c) Summary of TNF- α release determined by ELISA from microglial cells without (CTL) or with exposure for 72 hr to 100 nM A β_{42} alone or treatment with PF or U0126 at indicated concentrations, 30 min prior to and during exposure to 100 nM A β_{42} , from 3 independent cell preparations. ***, $p < 0.005$ compared to control. ###, $p < 0.005$ compared to cells exposed to A β_{42} alone.

Fig. 9 The PYK2/MEK/ERK signalling pathway is important in A β_{42} -induced activation of PARP-1 and TRPM2 channel

(a, b) *Left*, representative immunofluorescent images showing PAR generation (top row: PAR staining fluorescence; bottom row: counterstaining with DAPI) in microglia cells after exposure for 8 hr to 100 nM A β_{42} alone or treatment with 1 μ M PF (a) or 3 μ M U0126 (b). *Right*, summary of A β_{42} -induced PAR generation in microglial cells treated with conditions shown on the left, from 3 independent cell preparations. (c, d) *Left*, representative single cell

Fluo4 fluorescence images showing the cytosolic Ca^{2+} levels (top row: Fluo4 fluorescence; bottom row: counterstaining with Hoechst) in microglial cells after exposure to 100 nM $\text{A}\beta_{42}$ without or with treatment with 1 μM PF (c) or 3 μM U0126 (d). *Right*, summary of $\text{A}\beta_{42}$ -induced cytosolic Ca^{2+} responses in microglial cells under indicated conditions, from 3 independent cell preparations. Scale bar: 40 μm . ***, $p < 0.005$ compared to control. ###, $p < 0.005$ compared to cells exposed to $\text{A}\beta_{42}$ alone.

Fig. 10 PKC and NOX are responsible for $\text{A}\beta_{42}$ -induced activation of PARP in TRPM2-KO microglial cells

(a-f) *Left*, representative immunofluorescent images showing PAR generation (top row: PAR staining fluorescence; bottom row: counterstaining with DAPI) in TRPM2-KO microglia cells after exposure for 8 hr to 100 nM $\text{A}\beta_{42}$ alone or treatment with 3 μM CTC (a), 3 μM DPI (b), 3 μM GKT (c), 30 μM Phox (d), 1 μM PF (e) or 3 μM U0126 (f). *Right*, summary of PAR generation in microglial cells under indicated conditions, from 3 independent cell preparations. Scale bar, 40 μm . ***, $p < 0.005$ compared control. ###, $p < 0.005$ compared to cells exposed to $\text{A}\beta_{42}$ alone.

Fig.11 Schematic summary of the mechanisms underlying $\text{A}\beta_{42}$ -induced TRPM2 channel activation in microglial cells leading to microglial activation of generation of $\text{TNF-}\alpha$

Exposure to $\text{A}\beta_{42}$ induces activation of protein kinase C (PKC) and NADPH oxidases (NOX), including NOX1/4 and NOX2, leading to generation of ROS. ROS stimulate activation of p(ADP-ribose) polymerase-1 (PARP-1) in the nucleus to generate ADP-ribose (ADPR). ADPR activates the TRPM2 channel, resulting extracellular Ca^{2+} influx to increase the cytosolic Ca^{2+} concentrations ($[\text{Ca}^{2+}]_c$). Intracellular Ca^{2+} stimulates the PYK2/MEK/ERK

signalling pathway to further enhance activation of PARP-1 and TRPM2 channel. TRPM2 channel activation is required for A β ₄₂-induced microglial activation and generation of tumour necrosis factor (TNF)- α , a key proinflammatory cytokine implicated in neuroinflammation in Alzheimer's disease.

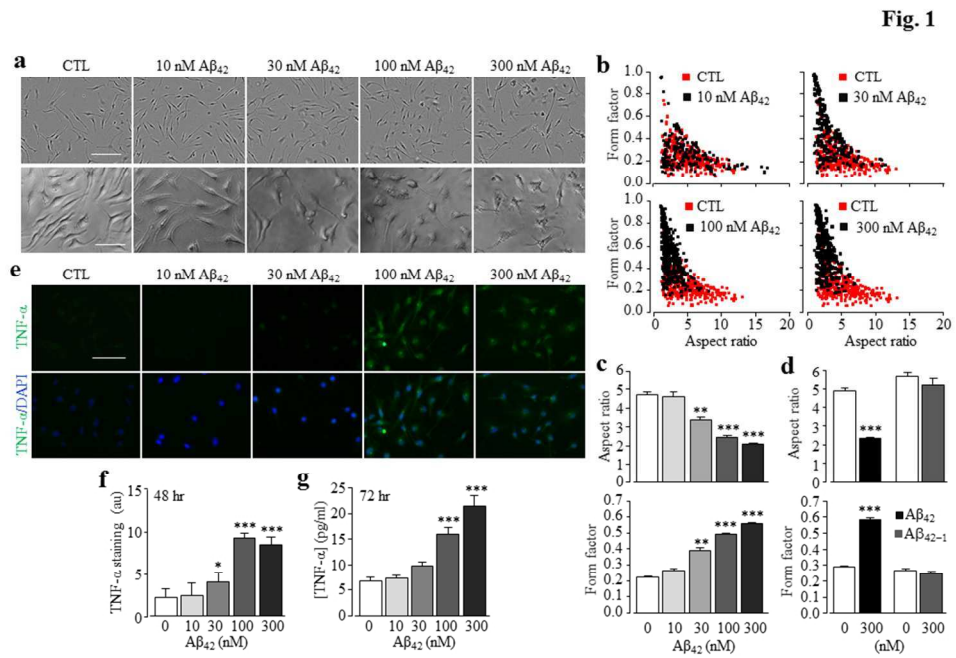


Figure 1

275x190mm (96 x 96 DPI)

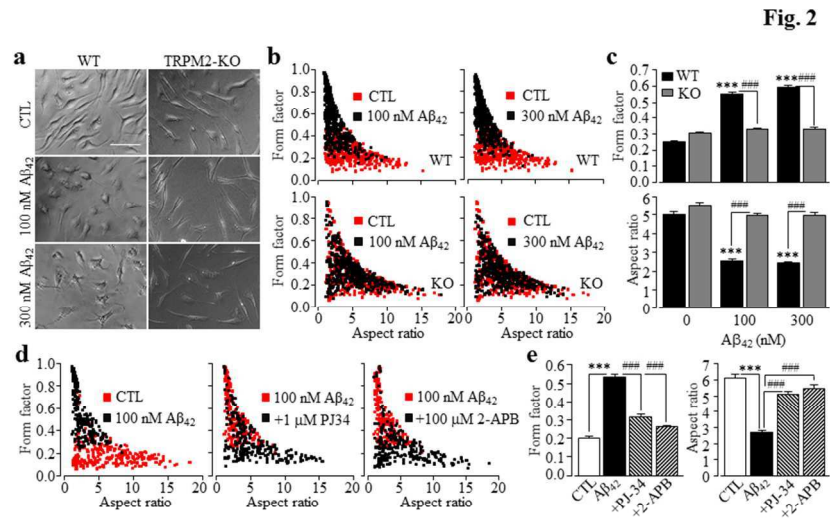


Figure 2

275x190mm (96 x 96 DPI)

Fig. 3

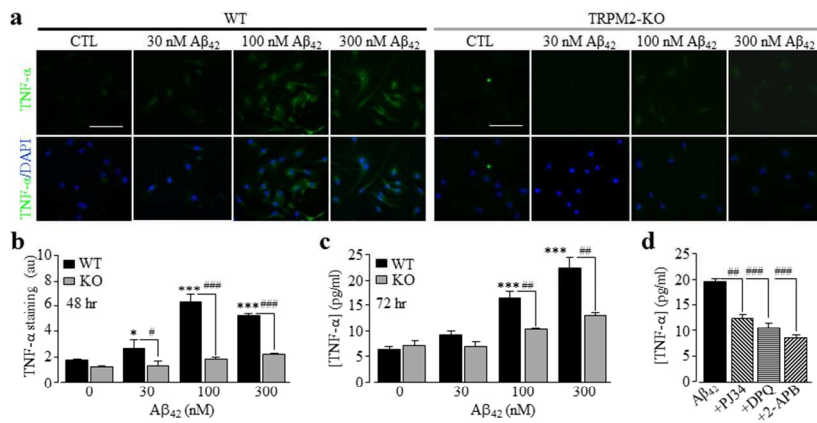


Figure 3

275x190mm (96 x 96 DPI)

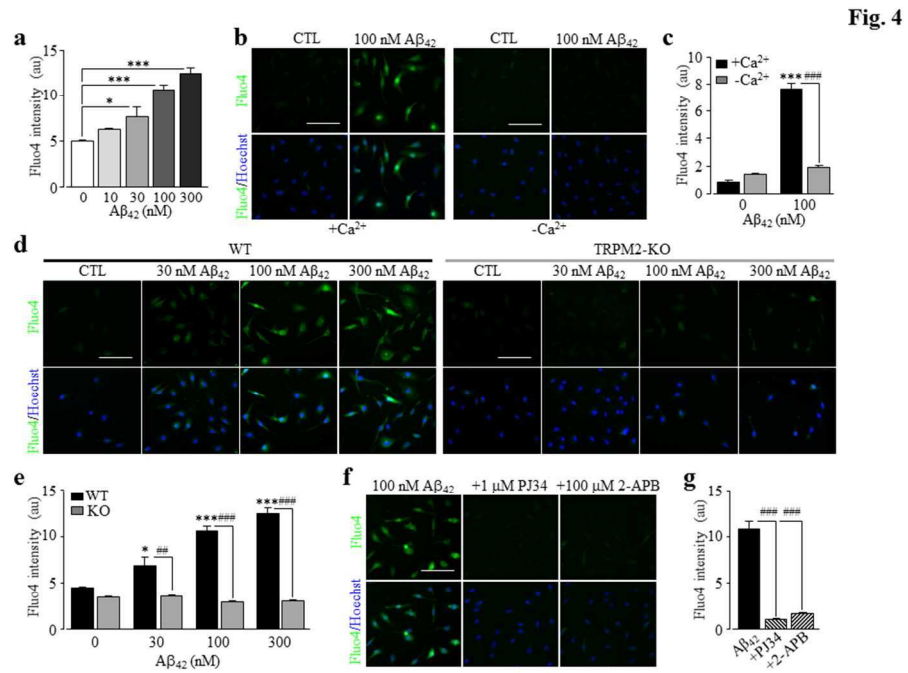


Figure 4

275x190mm (96 x 96 DPI)

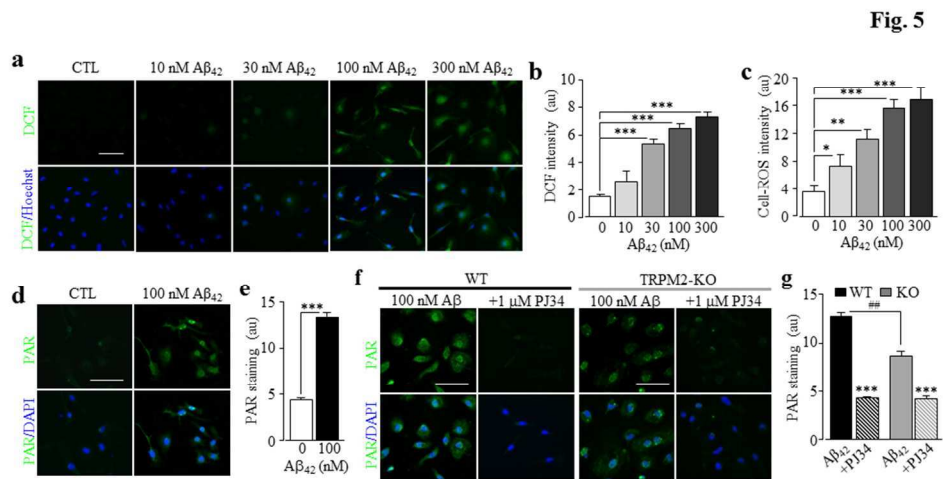


Figure 5

275x190mm (96 x 96 DPI)

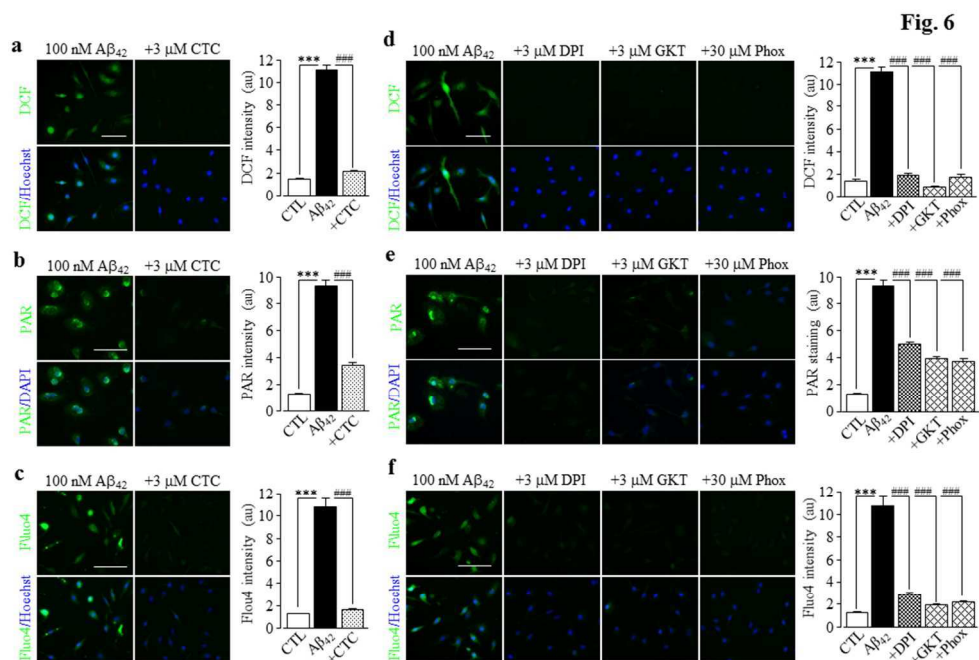


Figure 6

275x190mm (96 x 96 DPI)

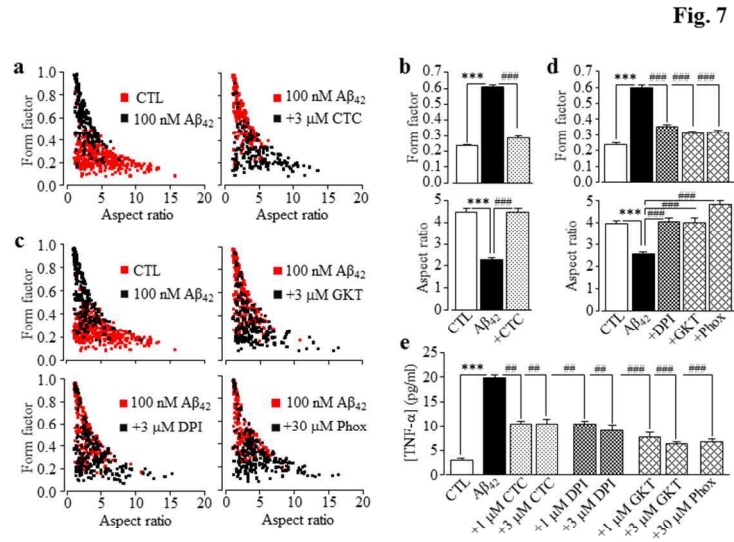


Figure 7

275x190mm (96 x 96 DPI)

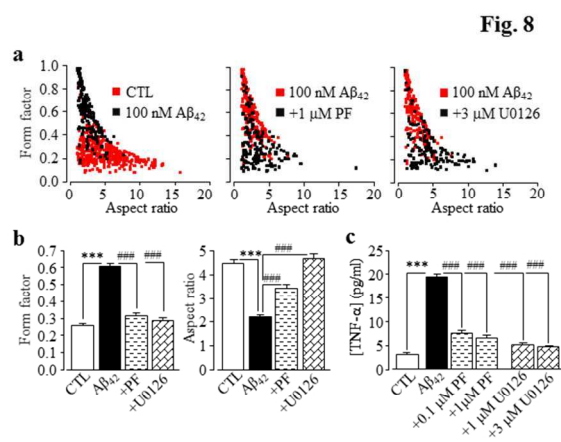


Figure 8

275x190mm (96 x 96 DPI)

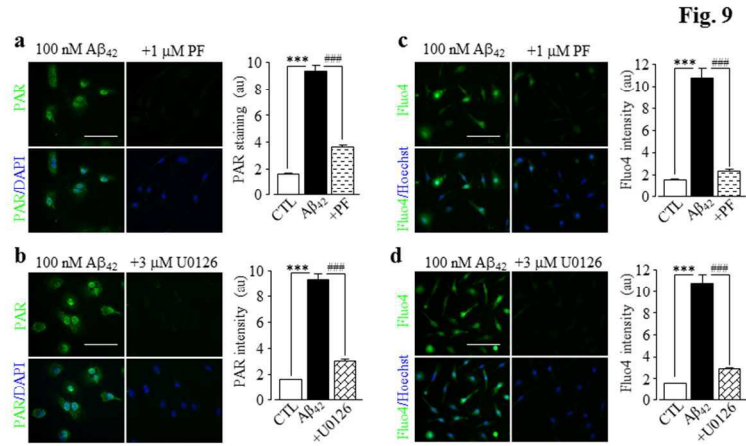


Figure 9

275x190mm (96 x 96 DPI)

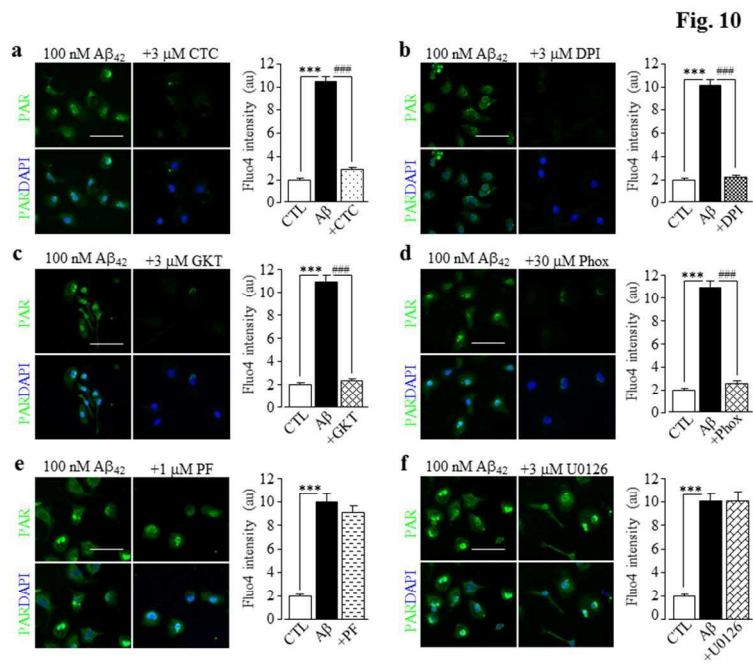


Figure 10

275x190mm (96 x 96 DPI)

Fig. 11

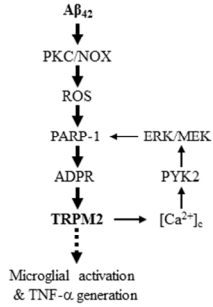


Figure 11

275x190mm (96 x 96 DPI)

Supporting information

A critical role of TRPM2 channel in A β ₄₂-induced microglial activation and generation of tumour necrosis factor- α

Sharifah Alawieyah Syed Mortadza, Joan A Sim, Veronika E Neubrand and Lin-Hua Jiang

Figure legend

Fig. 1 Control peptide A β ₄₂₋₁ induces no change in microglial cell morphology

Top, representative phase-contrast images showing cell morphology of microglial cells without (CTL) or with exposure for 24 hr to 300 nM A β ₄₂ (a) or 300 nM A β ₄₂₋₁ (b), captured using an EVOS image system with a 40x object lens. Scale bar, 50 μ m. *Bottom*, scatter plot showing the distribution form factor and aspect ratio values for individual microglial cells under indicated conditions, from 3 independent experiments using 3 well of cells for each conditions in each time.

Fig. 2 Exposure to A β ₄₂ induces no microglial cell death

(a) Representative fluorescent images showing propidium iodide (PI) staining of microglial cell death without (CTL) or with exposure to A β ₄₂ at indicated concentrations for 72 hr (top row: PI-stained dead cells; bottom row: all cells stained with Hoechst). (b) Summary of mean percentage of PI-positive cells, from 3 independent experiments using 3 wells of cells for each condition in each time.

Fig. 3 Control peptide A β ₄₂₋₁ induces no Ca²⁺ response in microglial cells

(a) Representative single cell Fluo4 fluorescence images showing the cytosolic Ca²⁺ levels in microglial cells without (CTL) or with exposure to A β ₄₂ at indicated concentrations for 8 hr (top row: Fluo4 fluorescence; bottom row: counterstaining with Hoechst). (b) Representative single cell Fluo4 fluorescence images showing the cytosolic Ca²⁺ levels in microglial cells (top row: Fluo4 fluorescence; bottom row: counterstaining with Hoechst) without (CTL) or with exposure for 8 hr to 300 nM A β ₄₂ (left) or 300 nM A β ₄₂₋₁ (right). (c) Summary of the mean Ca²⁺ responses in microglial cells under indicated conditions, from 3 independent

experiments using 3 wells of cells for each condition in each time. Scale bar: 40 μm . ***, $p < 0.005$ compared to control.

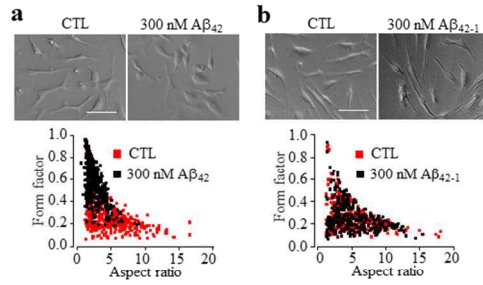
Fig. 4 $\text{A}\beta_{42}$ induced generation of ROS in microglial cells

Representative single cell Cell-ROX fluorescent images of showing cellular ROS production (top row: Cell-ROX fluorescence; bottom row: counterstaining with Hoechst) in WT microglial cells without (CTL) or with exposure to $\text{A}\beta_{42}$ at indicated concentrations for 8 hr.

Fig. 5 TRPM2 channel in $\text{A}\beta_{42}$ -induced ROS generation in microglial cells

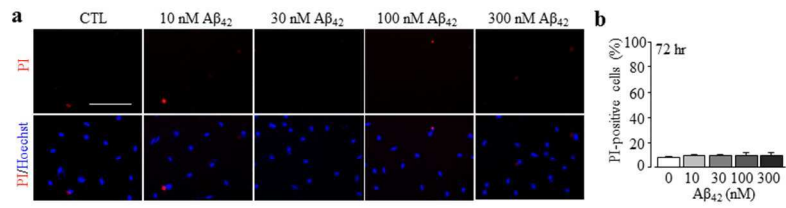
(a) Representative single cell Cell-DOX fluorescence images showing cellular ROS production (top row: Cell-ROX fluorescence; bottom row: counterstaining with Hoechst) in WT and KO-TRPM2 microglial cells without (CTL) or with exposure to $\text{A}\beta_{42}$ at indicated concentrations for 8 hr. (b) Summary of $\text{A}\beta_{42}$ -induced ROS production in microglial cells under conditions shown in (a) from 3 wells of cells (in triplicate) for each condition. Scale bar: 40 μm . *, $p < 0.05$; **, $p < 0.01$; ***, $p < 0.005$ compared to control. ##, $p < 0.01$; ###, $p < 0.005$ compared between WT and TRPM2-KO cells under the same treatment.

Supplementary Fig. 1



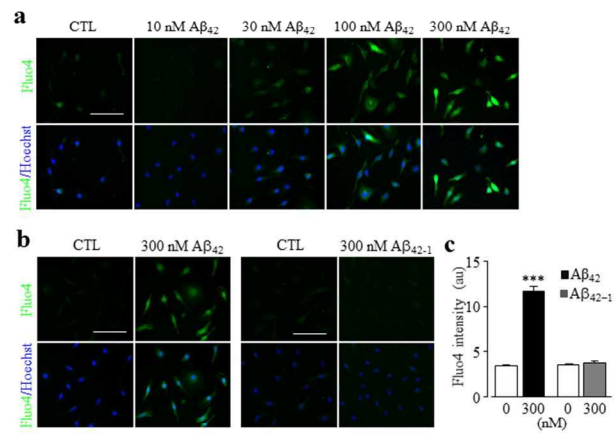
275x190mm (96 x 96 DPI)

Supplementary Fig. 2



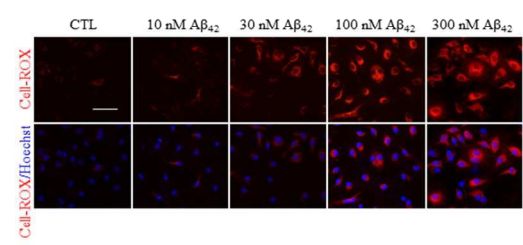
275x190mm (96 x 96 DPI)

Supplementary Fig. 3



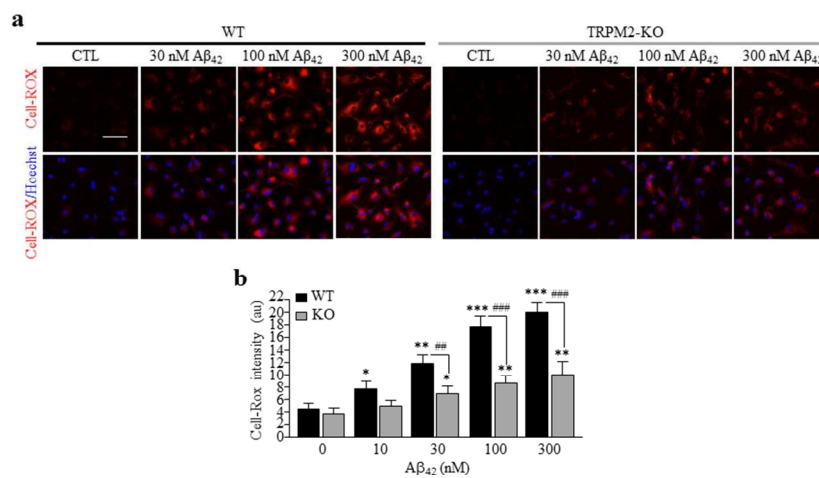
275x190mm (96 x 96 DPI)

Supplementary Fig. 4



275x190mm (96 x 96 DPI)

Supplementary Fig. 5



275x190mm (96 x 96 DPI)